

Seasonal Source Identification And Source-Specific Health Risk Assessment of Pollutants On Road Dust In Tianjin

Jingshu Wang

Nankai University

Jinhui Jeanne Huang (✉ Huangj@nankai.edu.cn)

Nankai University <https://orcid.org/0000-0002-5268-1747>

Catherine Mulligan

Concordia University

Research Article

Keywords: Road dust, Heavy metals, Source apportionment, Risk assessment, Seasonal source-specific risks

Posted Date: July 29th, 2021

DOI: <https://doi.org/10.21203/rs.3.rs-681169/v1>

License:  This work is licensed under a Creative Commons Attribution 4.0 International License.

[Read Full License](#)

Version of Record: A version of this preprint was published at Environmental Science and Pollution Research on September 12th, 2021. See the published version at <https://doi.org/10.1007/s11356-021-16326-8>.

1 **Seasonal source identification and source-specific health risk**
2 **assessment of pollutants on road dust in Tianjin**

3 Jingshu Wang^a, Jinhui Jeanne Huang^{a*}, and Catherine Mulligan^b

4
5
6 ^a College of Environmental Science and Engineering/Sino-Canada Joint R&D Centre
7 on Water and Environmental Safety, Nankai University, 300071, Tianjin, China

8 ^b Department of Building, Civil and Environmental Engineering, Concordia
9 University, Montreal, Quebec H3G 1M8, Canada

10
11
12 **Corresponding author: Jinhui Jeanne Huang**

13 Sino-Canada R&D Centre on Water and Environmental Safety, College of
14 Environmental Science and Engineering, Nankai University, Tianjin 300071, PR China;

15 Phone: (86)22-8535-8816; Fax: (86)22-8535-8816; E-mail: huangji@nankai.edu.cn

16 **Abstract**

17 Human exposure to metals on road dust might have potential health risks through
18 touching, ingesting, and inhaling. There were limited studies to link seasonal emission
19 sources to health risks from metals on road dust. In this study, metals on road dust from
20 different functional areas were seasonally monitored. The pollutant sources in study
21 city varied slightly with the seasons, but the major pollutant source in the particular
22 study site were significantly affected by the seasons. By combining the source
23 apportionment model (PMF), line sources model and health risk models (HI: Hazard
24 index and ILCR: Incremental Lifetime Carcinogenic risk), industrial and construction
25 activity was identified as the crucial source of both the pollutants on road dust (29% -
26 47%), and the HI for adults (27% - 45%) and children (41% - 50%) in different seasons.
27 The traffic non-exhaust emission dominated in the carcinogenic risks for children in
28 spring (45%) and summer (36%). Factors such as seasons, particle size, metal
29 bioavailability, human exposure time, and exposure area were all taken into
30 consideration to avoid overestimating or underestimating health risks. The carcinogenic
31 risks for children ($1.6 \text{ E-}06$) and adults ($2.8 \text{ E-}06$) exposed to Cr both exceed the
32 minimum threshold (10^{-6}). Measured metals mainly posed hazard to human health
33 through ingestion route. Pb and Mn, Fe and Mn were the main harmful elements that
34 induced non-carcinogenic risks for adults and children, respectively. Effectively
35 identifying the source-specific health risks in different seasons will help in the
36 formulation of adaptive strategies to diminish the potential risks.

37

38 **Keywords**

39 Road dust, Heavy metals, Source apportionment, Risk assessment, Seasonal source-

40 specific risks

41 **Introduction**

42 Pollutants on road dust can be measured as a comprehensive indicator of urban
43 pollution level (Dietrich et al., 2019; Skrbic et al., 2019; Wahab et al., 2020; Živančev
44 et al., 2019). Metals are prevalent on the road surface and build up on the road dust
45 from multiple pollution sources by natural or human activities. The accumulation of
46 road dust itself also serve as a notable pollutant source (Tian et al., 2019). Road dust
47 can be transported into the drainage systems by runoff, and the associated pollutants
48 could reach receiving water body and adversely affect the water ecosystem (Gavrić et
49 al., 2019); it could also be resuspended into the atmosphere by wind or vehicle
50 movement, affecting air quality and threatening human health (Pateraki et al., 2019).
51 The source analysis of the atmospheric particles in Tianjin reported by the former
52 Ministry of Environmental Protection indicated that road dust was the vital source
53 accounting for 30% of the PM_{2.5} (particles with an aerodynamic equivalent diameter of
54 2.5 microns or less) (Zhao et al., 2019). The key to reducing the adverse effects of road
55 dust is to quantitatively identify and evaluate its pollution sources and risks (Men et al.,
56 2020). Many studies have emphasized that the pollution sources might vary in different
57 seasons, but there is a lack of detailed supporting data (Liu et al., 2015; Men et al.,
58 2020).

59 Source apportionment was extracted by the receptor model, and the source
60 contribution to the contaminants on road dust was quantified mathematically based on
61 the source composition or fingerprint. Many studies have applied the receptor model,
62 such as multiple linear regression (PCA-MLR) (Zhang et al., 2019b), principal

63 component analysis (PCA) (Asheim et al., 2019), factor analysis (FA) (Bzdusek et al.,
64 2004), positive matrix factorization (PMF) (Men et al., 2019), and forward stepwise
65 regression (FSWR) (Liu et al., 2018) to evaluate and identify the possible sources of
66 target pollutants in air (Wang et al., 2018), soil (Wang et al., 2019b) and water (Salim
67 et al., 2019; Škrbić et al., 2018). This has accumulated a lot of knowledge on the source
68 tracking of pollutants such as polycyclic aromatic hydrocarbons (Skrbic et al., 2019)
69 and metals (Wang et al., 2019b). Obviously, different models have different advantages
70 and disadvantages (Huang et al., 2018c). In order to quantitatively analyze the
71 contribution proportion of pollution sources on metals and human health risks, the PMF
72 model was selected in this study (Men et al., 2019). This model considers the
73 uncertainty of sampling and data analysis, and could quantify the source contribution
74 to meet the research goals.

75 The metals, such as Fe, Mn, Pb, Zn, Cr and Cu, are ubiquitous on road dust and
76 have potential adverse effects on human health, including cell injury, inflammation or
77 heart diseases (Huang et al., 2018b; Men et al., 2020). The Hazard Index (HI) model
78 was selected to assess the potential non-carcinogenic risk of human exposure to metals
79 (Wahab et al., 2020). Adults and children exposed to the road dust made pollutants
80 easier to enter the human body through three pathways: ingestion (exposure of mouth
81 and digestive tract), inhalation and dermal contact (Skrbic et al., 2019). Cr and Pb were
82 not the essential elements for living and showed higher toxic to animals, plants and
83 human beings (Wahab et al., 2020). The Incremental Lifetime Carcinogenic risk (ILCR)
84 model was used to assess the carcinogenic risks of Cr and Pb to human health which

85 has been widely applied in many studies (Liu et al., 2015). However, in previous studies,
86 a common practice in calculating the daily exposure dose (ADD) of road dust through
87 the inhalation route was to classify it as soil using a particulate emission factor (PEF)
88 (Hou et al., 2019). This might underestimate the amount of inhalation or ingestion,
89 because it ignored the impact of particle size and severe traffic disruption.
90 Comprehensive and mature models have been developed in air pollution simulation,
91 including NORTRIP, and AERMOD (Tian et al., 2019). Although these methods were
92 valuable, they require a large number of parameters like road condition and climate
93 with large calculation costs. This study was the first attempt to combine the road dust
94 emission model AP-42 (EPA, 2001b) with linear model, representing the pollutant
95 diffusion, to obtain a relatively accurate estimate of suspended road dust. Furthermore,
96 season was often overlooked in the risk assessment. According to the Exposure Factors
97 Handbook of Chinese Population (Ministry of Ecology and Environment, 2013), the
98 exposure time and exposure area of people varied in different seasons, which would
99 affect the accuracy of the risk assessment.

100 Accurate source control is the key to mitigating the health risks of metal exposure.
101 Affected by the characteristics of the functional areas and seasons, this study
102 emphasized that the seasonal sources of pollutants in each functional area might be
103 significantly distinctive. In addition, many studies have focused on the source
104 apportionment of pollutants on road dust, but ignored the crucial sources leading to
105 health risks (Men et al., 2020). Due to the different toxic reaction factors of metals, the
106 major sources of metals on road dust might not generate the major risks to human health

107 (Liu et al., 2015). And the crucial sources of health risks might also be affected by the
108 seasons. The combination of the PMF model and the risk assessment model could
109 achieve accurate and effective evaluation of the source apportionment of health risks.

110 In order to mitigate hazardous pollutants on road dust effectively, the objectives of
111 this work contained four items: 1) investigate the pollution characteristics of metals on
112 road dust in different functional areas and seasons; 2) identify the vital pollution sources
113 of measured metals on road dust in different seasons; 3) evaluate the carcinogenic and
114 non-carcinogenic risks of metals on road dust for different human groups (adult and
115 children) through three pathways in different seasons and functional areas; 4)
116 distinguish the crucial sources of health risks. This study on the source-specific risk
117 assessment of metals on road dust could provide a theoretical basis and guidance in
118 controlling the potential risks to human health.

119 **1. Materials and Methods**

120 **1.1 Sampling site**

121 Tianjin is a typical metropolis with an area of 11966.45 km² and a population more
122 than 15.6 million, and it is a largest port city in northern China. There were few studies
123 on the metals on road dust and its potential risks to human health in Tianjin recently
124 (Živančev et al., 2019). Hexi District, as one of the administrative districts in the city
125 center, was selected in this research. Tianjin has a typical warm and semi-humid
126 continental monsoon climate with distinct seasons: hot and rainy summer, and cold and
127 dry winter. The relatively large wind speed appears in the spring and winter, and the
128 average wind speed is about 2 m·s⁻¹ throughout the year (Wang et al., 2019a). Each

129 functional area exhibited different regional characteristics. Four typical areas, traffic
130 areas (JT), commercial areas (SY), residential areas (JM), and central commercial
131 streets (BJ) (with more intensive business activities, people and traffic volume than JM),
132 were selected in this study due to the significant differences in the population and traffic
133 volume as shown in Figure S1 and Table S1. There were large construction activities
134 near the traffic area during study period.

135 **1.2 Sampling and measurement**

136 In this work, three sampling spots were set at each study area for each sampling
137 event. The detailed sampling process and pretreatment methods were performed
138 according to our previous work as shown in SI (Wang et al., 2020). The survey duration
139 included four quarters, started from December 2016 to November 2017, and the
140 detailed sampling date was displayed in Table S1. Thereout, an average of 15 samples
141 was taken each quarter at each site, and a total of 240 samples were obtained in four
142 study areas. The pretreated samples were further sieved into three groups of particles
143 with size $<75\ \mu\text{m}$, $75\text{-}150\ \mu\text{m}$, and $150\text{-}500\ \mu\text{m}$. The particles with different sizes might
144 pose threat to human health in different pathway. Many studies have found that
145 different size particles have various behavioral characteristics (Gbeddy et al., 2018;
146 Wang et al., 2019a; Wijesiri et al., 2016). Fine particles ($<75\ \mu\text{m}$) were more likely to
147 be suspended into the air and endangered human health through inhalation (Deletic and
148 Orr, 2005; Tomašević et al., 2005). While coarse particles might be more inclined to
149 cause health risks through dermal contact or ingestion (Zhao et al., 2016). Therefore,
150 metals in different size particles (Table S2) were evaluated for risks through three

151 pathways.

152 Metals (Fe, Mn, Pb, Zn, Cr, Cu) in size-fractioned particles were analyzed using
153 the microwave acid extraction with Agilent-7800 ICP-MS instrument system. The
154 nutrients (NH₃-N, NO₃⁻-N, TOC and TP) in the samples were extracted and measured
155 according to the China standard methods (HJ 535-2009, GB/T 32737-2016, HJ 632-
156 2011) (SI). NH₃-N, NO₃⁻-N, TOC and TP, as nutrients, were considered to obtain more
157 accurate source apportionment results. The analysis process of elements conformed to
158 the quality assurance and quality control (QA/QC) procedures and the detailed
159 information was shown in SI.

160 **1.3 Positive matrix factorization (PMF) model**

161 PMF 5.0 was selected for source apportionment in this study (Paatero and Tapper,
162 1994). The positive matrix factorization (PMF) model employs non-negative
163 constraints to quantify the contribution of potential sources to the samples, and
164 considers the error estimation. It overcomes the occurrence of unexplained factors such
165 as non-negative factors that are prone to appear in other receptor models such as
166 principal component analysis (PCA). PMF analyzes source factors by a weighted least-
167 squares fit method (Zhang et al., 2019b). Positive matrix factorization analysis comes
168 with bootstrap uncertainty analysis, which is the best choice for quantitative analysis of
169 pollutant sources.

170 PMF is a multivariate factor analysis tool that decomposes a matrix of speciated
171 sample data into two matrices: factor contributions (G) and factor profiles (F). These
172 factor profiles need to be interpreted by researchers to identify the source types that

173 may be contributing to the samples using measured source profile information, and
 174 emissions or discharge inventories. As input files, data set can be viewed as a data
 175 matrix X of i by j dimensions, in which i number of samples and j chemical species
 176 were measured, with uncertainties u . The goal of receptor models is to solve the
 177 chemical mass balance (CMB) between measured species concentrations and source
 178 profiles, as shown in Eq. (1), with number of factors p , the species profile f of each
 179 source, and the amount of mass g contributed by each factor to each individual sample:

180

$$181 \quad x_{ij} = \sum_{k=1}^p g_{ik} f_{kj} + e_{ij} \quad \text{Eq. (1)}$$

182 where e_{ij} is the residual for each sample/species.

183 The residual error matrix e_{ij} is calculated by the minimum value of the objective
 184 function Q in Eq. (2):

$$185 \quad Q = \sum_{i=1}^n \sum_{j=1}^m \left(\frac{e_{ij}}{u_{ij}} \right)^2 \quad \text{Eq. (2)}$$

186 where u_{ij} is the data uncertainty calculated using a fixed fraction of the species-
 187 specific method detection limit (MDL) (Men et al., 2020; Wang et al., 2019b).

188 Q is a critical parameter for PMF with two versions of Q , $Q(true)$ and $Q(robust)$,
 189 providing the assessment of model stability. To run the model, it requires the proper
 190 species concentration and uncertainty files. The uncertainty was calculated using the
 191 following Eqs. (3-4):

$$192 \quad \text{If concentration} < MDL, \quad u_{ij} = \frac{5}{6} \times MDL \quad \text{Eq. (3)}$$

$$193 \quad \text{Otherwise,} \quad u_{ij} = \sqrt{(Error \ Fraction \times \ concentration)^2 + (0.5 \times MDL)^2} \quad \text{Eq.}$$

$$194 \quad (4)$$

195 Where concentration is the content of species, *MDL* and Error Fraction (relative
196 standard deviation) are shown in Table S3.

197 The signal-to-noise ratio (S/N) of all elements was >1.0. The values of scaled
198 residuals for all the elements were between -3 and +3, and were normally distributed.
199 The model Q (robust) and Q (true) values were fitted and compared, and the difference
200 was less than 3% which meant the model run stably and the data fit well. The standard
201 error (*SE*) between the observed and predicted values was less than 0.1. Through
202 Bootstrapping (BS) and Displacement (DISP) error estimation, the uncertainty of
203 model could be explained and accepted, and the number of factors was also appropriate.

204 **1.4 Human exposure and health risk assessment**

205 Based on the US Environmental Protection Agency health risk handbook (EPA,
206 2001a), the exposure assessment model was used to assess the potential risks of toxic
207 elements on road dust to human health. According to the model, people exposed to
208 metals on road dust could occur through three main pathways: direct ingestion (ADD_{ing}),
209 dermal absorption (ADD_{der}) and inhalation (ADD_{inh}) (Rahman et al., 2019). The
210 average daily dose received by adults and children was evaluated by formula
211 calculation (Zhao et al., 2014). The parameters in the numerical expressions of cancer
212 and non-cancer risk assessments for humans was selected from the US Environmental
213 Protection Agency health risk handbook (EPA, 2001a; 2004; 2009a) and the Exposure
214 factors handbook of Chinese Population (Ministry of Ecology and Environment, 2013).
215 The potential health effects of metals were described as non-carcinogenic and
216 carcinogenic risks according to the exposure assessment. The non-carcinogenic risks of

217 six metals to human health were evaluated by the Hazard Index (HI) and Hazard
218 Quotient (HQ) (Bourliva et al., 2016; Zheng et al., 2010). According to the Agents
219 Classified by the International Agency for Research on Center (IARC) Monographs, Cr
220 and Pb were carcinogenic hazards to humans and the associated carcinogenic risk were
221 assessed by Incremental Lifetime Carcinogenic risk (ILCR).

222 The particle emission factors from soil in the risk assessment model were replaced
223 by the emission of road fugitive dust to avoid underestimating potential health risks
224 (Tian et al., 2019). The AP-42 model (U.S. EPA, 2001) and the Line Sources model
225 were used to evaluate the particle emissions from road surface in different functional
226 areas, and the detailed model was displayed in the SI. The relative bioavailability (RBA)
227 of metals, which represented the bioavailability fraction of the metal content (%), was
228 also essential to avoid overestimating health risks (Table S4) (Hou et al., 2019). Due to
229 the limitations of experimental conditions, the ratio of metal bioavailability was
230 referred to previous research results in Tianjin (Hou et al., 2019; Hu et al., 2011; Yu et
231 al., 2014). In addition, the exposure time and body exposure area of people in different
232 seasons were also considered into the model in this study.

233 1.4.1 Exposure dose

234 The daily intake dose (ADD) of each metal through three pathways was calculated by
235 using Eqs (5-7).

$$236 \quad ADD_{ing} = C \times \frac{IngR \cdot ET \cdot EF \cdot ED}{BW \cdot AT_{non}} \times$$

237 10^{-6} Eq. (5)

$$238 \quad ADD_{inh} = C \times \frac{InhR \cdot ET \cdot EF \cdot ED \cdot RED}{BW \cdot AT_{non}} \times$$

239 10^{-9} Eq. (6)

240
$$ADD_{der} = C \times \frac{AF_d \cdot SA \cdot ABS \cdot ET \cdot EF \cdot ED}{BW \cdot AT_{non}} \times$$

241 10^{-6} Eq. (7)

242 Where, ADD is the average daily dose through three routes (mg/(kg·day)). *C* in
 243 Eqs. (5-7) is the metal concentrations on road dust in mg/kg. *IngR* is the ingestion rate
 244 of road dust in mg·day⁻¹. *InhR* is the inhalation rate in m³·day⁻¹. *ET* is the exposure time
 245 of day (h/d). *EF* is the exposure frequency in day/year. *ED* is the exposure duration,
 246 years. *RED* is the exposure dose of road dust suspended from the road surface in ug/m³.
 247 *SA* is the exposed skin area in cm². *AF_d* is the skin adherence factor in mg·cm⁻²·day⁻¹.
 248 *BW* is the body weight of human and child in kg. *AT* is the average exposure time in
 249 hours (h). *ABS* is the dermal absorption factor (unitless). The parameters are shown in
 250 Table S4a.

251 1.4.2 Hazard index (HI)

252 HQ and HI values can be calculated by the following equations (8-12) from EPA
 253 guidance documentation to assess the health risks with a threshold pollutant (EPA):

254
$$HQ_{ing} = \frac{ADD_{ing} \cdot RBA}{RfD_{ing}} \quad \text{Eq. (8)}$$

255
$$HQ_{inh} = \frac{ADD_{inh} \cdot RBA}{RfD_{inh}} \quad \text{Eq. (9)}$$

256
$$HQ_{der} = \frac{ADD_{der} \cdot RBA}{RfD_{der}} \quad \text{Eq. (10)}$$

257
$$HI = \sum_1^i HQ \quad \text{Eq. (11)}$$

258
$$HI_x = HI_x \quad \text{Eq. (12)}$$

259 Where, *i* is the exposure pathway. *x* is the relevant metal species. *RfD* is the
 260 reference permissible daily intake dose in mg/(kg·d) for ingestion and dermal contact

261 or mg/m^{-3} for inhalation. Relative bioavailability (*RBA*) of the metals was shown in
 262 Table S4b. The HQ calculated for each exposure route was added to obtain HI to assess
 263 the potential non-carcinogenic risk effects of specific metal. HI was used to estimate
 264 non-carcinogenic risks for multiple metals (Zhang et al., 2019a). HI value less than 1
 265 suggests no significant non-carcinogenic risk.

266 1.4.3 Incremental Lifetime Carcinogenic risk (ILCR)

267 Pb and Cr, as non-threshold contaminants, were assessed by the Incremental
 268 Lifetime Cancer Risk (ILCR) for the carcinogenic risk (CR) effect. It was used to
 269 measure the probability of carcinogenic risk during a 70-year lifetime continuous metal
 270 exposure. It was calculated using Eqs. (13-15):

$$271 \quad LADD_{inh} = \frac{C \cdot ET \cdot EF \cdot RED}{AT_{car}} \times \left(\frac{InhR \cdot ED}{BW} \right)_{child} \quad \text{Eq. (13)}$$

272

$$273 \quad LADD_{inh} = \frac{C \cdot ET \cdot EF \cdot RED}{AT_{car}} \times \left(\frac{Ingh \cdot ED}{BW} \right)_{adult} \quad \text{Eq. (14)}$$

274

$$275 \quad ILCR = LADD \times RBA \times SF \quad \text{Eq. (15)}$$

276 Where, *ILCR* is the incremental lifetime cancer risk. *LADD* is the lifetime average
 277 daily dose exposed by the inhalation pathways ($\mu\text{g}/\text{m}^3$). *ET* is the exposure time (h/d).
 278 *SF* is the cancer slope factor. Carcinogenic risks in the range of 1.0×10^{-6} to 1.0×10^{-4}
 279 were considered non-negligible and should be controlled through risk management
 280 decisions (Tian et al., 2019).

281 1.4.4 Source contribution for risk assessment

282 According to the source apportionment resulted from the PMF model, the new

283 combination of PMF - ILCR was used to assess the source contribution to human health
284 risks, which was calculated as follows:

$$285 \quad S[ILCR]_{jk} = S[LADD]_{jk} \cdot SF \quad \text{Eq. (16)}$$

$$286 \quad S[HQ]_{jk} = \frac{S[ADD]_{jk} \cdot RBA}{RfD} \quad \text{Eq. (17)}$$

$$287 \quad SC_{jk} = C_j \cdot S_k \quad \text{Eq. (18)}$$

288 Where, $S[ILCR]_{jk}$ and $S[HQ]_{jk}$ is the risk exposed in the j th metal and contributed
289 by the k th pollution source for carcinogenic and non-carcinogenic effects, respectively.
290 $S[LADD]_{jk}$ and $S[ADD]_{jk}$ is the average daily dose of the j th metal contributed by the
291 k th pollution source (mg/kg/d). C in Eqs. (5-7) and Eqs. (13-15) presenting metal
292 concentration is replaced by SC_{jk} . C_j is the j th metal concentration in road dust (mg/kg).
293 S_k is the contribution proportion of the k th source to the metal concentration (%). SF is
294 the cancer slope factor, and RBA is the relative bioavailability of metal which shown in
295 Table S4b.

296 **1.5 Statistical analysis**

297 The figures and data analysis in this study were completed in the GraphPad Prism
298 8 software. The concentration difference of metals on road dust between different
299 seasons is expressed by coefficient of variation (CV) and the equation is as follows:

$$300 \quad CV = \frac{sd}{mean} \times 100\%$$

301 **2. Results and discussion**

302 **2.1 Concentration characteristics of heavy metals on road dust**

303 Figure 1 displays the seasonal concentration distribution of metals in functional
304 areas. The concentrations of Fe and Mn in both the traffic area (JT) and the residential

305 area (JM) were relatively higher except in spring. While the concentrations of Pb, Zn,
306 and Cr were prominent in the commercial area (SY) and the central commercial street
307 (BJ). The concentration of Cu in different sites was most affected by the season, with
308 the highest concentration in commercial area (SY) in spring and autumn, but the highest
309 concentration in residential area (JM) in summer and the highest concentration in the
310 central commercial street (BJ) in winter. Obviously, the metal concentrations were
311 significantly affected by the ambient environment of different functional areas (Huang
312 et al., 2018a). A pronounced seasonal variation was also observed in metal
313 concentration distributions. The concentrations of most metals were lower in spring,
314 but higher in other seasons. Many studies have confirmed the seasonal differences in
315 metal concentration (Men et al., 2018). The concentrations of Fe, Mn, Pb and Cu varied
316 greatly among functional areas in summer with a large Coefficient of Variation (CV),
317 while the concentrations of Zn and Cr differed significantly among functional areas in
318 autumn (Table S5). This might be related to the extensive human activities in summer
319 and autumn, like construction activities and industrial activities (Skrbic et al., 2019).

320 Compared with metals Zn, Cr, Cu, and Pb, metals Fe and Mn were found to have
321 the highest concentrations on road dust. The average concentrations of Fe and Zn in
322 most areas were more than five times of the soil background value in Tianjin (Table S6),
323 and the concentrations of Pb and Cu on road dust were more than twice (CNEMC).
324 While the concentrations of Mn and Cr in most areas were lower than the background
325 values. The concentration of Mn was similar to that in other cities of China, but it was
326 higher than that in London and lower than that in Honolulu (Robertson et al., 2003;

327 Sutherland and Tolosa, 2000). Compared with the metal concentrations studied in other
328 cities in China or other countries (Table S6), the concentration of Fe in this study area
329 was significantly lower than that in Beijing (Men et al., 2020), but it was close to the
330 findings in Ottawa Canada and Queensland Australia (Gunawardana et al., 2014;
331 Rasmussen et al., 2001). The concentration of Pb in study areas was similar to
332 Birmingham UK (Charlesworth et al., 2003), but significantly lower than that in other
333 cities such as New York US, Tokyo Japan and Bhopal India, and Chinese cities such as
334 Shanghai and Xi'an (Banerjee, 2003; Fergusson and Ryan, 1984; Shi et al., 2008;
335 Wijaya et al., 2012; Yongming et al., 2006). The concentration of Zn in study areas was
336 comparable to the survey results of most cities in the world. The concentrations of Cu
337 and Cr were lower than those in the cities of China, but higher than those in Ottawa
338 Canada (Rasmussen et al., 2001). This might affect by factors such as the geological
339 conditions, economic development and intensity of human activity in different cities,
340 which need further research (Hou et al., 2019).

341 **2.2 Seasonal and regional source identification**

342 A receptor model (PMF) has been widely used to identify and quantify the main
343 sources of elements on road particles. However, the contribution of the sources to the
344 elements which might affected by the seasons, was not well studied in previous
345 literature (Men et al., 2020). Five major factors were identified for the elements on road
346 dust in different seasons, including atmosphere deposition, fertilizer, domestic waste,
347 industrial and construction activity, and traffic non-exhaust emission. The contribution
348 ratios of factors to different elements on the road dust were calculated by Eq. 1.

349 The contributions of factors to the elements on road dust in different seasons are
350 shown in Table 1. The first factor was characterized by a high contribution of $\text{NO}_3\text{-N}$
351 which does not depend on the seasons. As an important component in the air, nitrogen
352 oxides might come from the burning of fossil fuels, or the natural behaviors in the
353 atmospheric environment (thunderstorms, photochemical reactions, etc.) (Giroux et al.,
354 1997; Lin et al., 2015). In recent years, the increasing nitrate in atmospheric particles
355 could accumulate on the road surface as sediment (Feng et al., 2021). Therefore, factor
356 1 was identified as atmosphere deposition. The second factor was dominated by $\text{NH}_3\text{-N}$
357 N (48.6%) in spring, while dominated by TP (53.2% - 61.3%) in summer, autumn and
358 winter. There are many green belts near or on the urban roads, and chemical fertilizer
359 can provide the necessary nitrogen and phosphorus elements for the trees (Salim et al.,
360 2019). The seasonal differences in the contributions of nitrogen and phosphorus to the
361 factor could be explained by the different types of fertilizer. Therefore, factor 2 was
362 identified as fertilizer. The third factor was contributed by total organic carbon (TOC).
363 Considering the characteristics of the study area, there are many commercial activities
364 in the commercial area, and daily life in the residential area, which will generate a lot
365 of domestic waste. Previous studies have found that the runoff from the residential area
366 has significant concentrations of organic carbon (Rhee et al., 2012; Salim et al., 2019).
367 Therefore, the factor 3 was identified as domestic waste. The fourth factor was mainly
368 characterized by Fe (41.6% - 50%) and Mn (42.4% - 50%) in four seasons. Even this
369 factor was also partly contributed by Pb, Cr and Cu in spring, Cr in summer, Cu and Zn
370 in autumn, Cu, Zn and Cr in winter. Fe, Mn and Cu were often used in industrial

371 activities such as electronic industry, mechatronics and construction (Men et al., 2020).
372 There are many industrial parks near the study area, thus the fine particles could release
373 into the environment by the wind and accumulate on the road surface. The fourth factor
374 was identified as industrial and construction activity. The fifth factor was dominated by
375 Pb (18% - 46.2%), Zn (26.9% - 51.4%) and Cr (29.6% - 44.1%). Cu could partly
376 contribute to the factor in spring and winter. Restricted use of leaded gasoline and diesel
377 has significantly reduced the content of Pb in vehicle exhaust emissions (Hong et al.,
378 2020). Pb, Zn, Cr and Cu were widely contained in brakes, tires, and pavements (Huang
379 et al., 2018b; Men et al., 2020). Therefore, the fifth factor was regarded as traffic non-
380 exhaust emission. The main sources (five factors) of measured elements in road dust in
381 study city were not affected by the seasons. However, the relative contribution percent
382 of each element to the factors varied significantly with seasons. Therefore, research on
383 the risk assessments of pollutant sources in specific season is more necessary.

384 Affected by different human activities, the source contribution percent in different
385 study sites is also fluctuant with seasons (Table S7). Due to the relatively higher green
386 area in residential areas (JM), fertilizer was a major source in different seasons. In
387 addition, atmospheric deposition was also an important source in summer and autumn,
388 while domestic waste and industrial activities were important sources in spring and
389 winter, respectively. For the traffic area (JT), construction activity was the major source
390 in spring, summer and autumn. This might be due to the large number of construction
391 activities beside the road during the study period. This source feature was consistent
392 with the characteristics of construction activities, which activities would decrease in

393 winter. Besides, domestic waste became the main source in winter. What was
394 interesting was that traffic non-exhaust emission is not an important source, even
395 though the traffic volume in the traffic area was very large. It was presumed that express
396 way had no traffic lights on the road, which reduced the abrasion of brakes, tires, and
397 pavement. Research indicated that traffic congestion could increase vehicle emissions
398 and reduce the air quality (Zhang and Batterman, 2013). Furthermore, the higher
399 contribution of construction activities to the measured elements on road dust made the
400 contribution of traffic non-exhaust emissions insignificant. Compared with the central
401 commercial street (BJ), commercial area (SY) had reduced business activities and
402 traffic volume. However, the vehicles were constantly braking at intersections due to
403 the narrow roads. As a result, non-exhaust emissions from traffic became the main
404 source in commercial area (SY) in different seasons. In addition, fertilizer and domestic
405 waste were also important sources of elements in autumn. Traffic non-exhaust emission
406 was the main source of central commercial street (BJ) in winter. Due to more
407 commercial activities and human flow, domestic waste became the main source in
408 spring and summer. The fertilizer and atmospheric deposition were also the main
409 sources in spring and autumn, respectively.

410 From the perspective of overall measured elements on road dust, the pollutant
411 sources in this study city did not vary with the seasons (Figure S2). However, the major
412 pollutant source in the particular study area were significantly affected by the seasons.
413 Seasons might indirectly affect the pollution sources of road dust by directly affecting
414 the economy activities, human activities, environmental policy, or other factors, which

415 need to be further studied.

416 **2.3 Seasonal non-carcinogenic risk health assessment**

417 The health risks of road dust were evaluated by summarizing the risks of different
418 groups of people exposed to metals on road dust in various functional areas and seasons.
419 Table S8 shows the Hazard Quotient (HQ) and Hazard Index (HI) for adults and
420 children exposed to six metals on road dust through three pathways. The potential health
421 risks of metals to adult in different seasons and functional areas are presented in Figs.
422 2-3. Figs. S3-S4 focus on the potential non-carcinogenic risk to children. $HI < 1$ was
423 considered to be free of non-carcinogenic risks. The results showed that the non-
424 carcinogenic risk for adults caused by a single metal through any exposure route or the
425 exposure to six metals was less than 1. It was confirmed that the target metals would
426 not pose a significant threat to the adult health. And the metals on road dust mainly
427 effected adult health through the ingestion route (Figure 2). Especially for metals Pb
428 and Mn, the HI values were 2.6×10^{-3} and 1.3×10^{-3} respectively. Although the evaluation
429 results were lower than the risk threshold, it still needed to pay more attention to these
430 two metals which often used in the construction activity and vehicle fabrication. Many
431 studies have implied that Mn was an important hazardous element and could cause a
432 higher non-cancer risk (Dietrich et al., 2019; Rahman et al., 2019; Tian et al., 2019). A
433 high concentration of Mn was determined in many cities in China (Sutherland and
434 Tolosa, 2000; Yang et al., 2010; Yongming et al., 2006), and it was also true in this
435 study. It is worth noting that the health risks induced by Mn need advanced
436 investigation based on the doses and concentration levels (Alves et al., 2017). Then, the

437 metals that caused the health risks were in the order of Zn>Fe> Cr > Cu. Excessive
438 intake of Fe might also have negative impacts on human health, although Fe was always
439 an essential element to human body. There have been many reports on the relationship
440 between excess iron and heart disease (Ghafourian et al., 2020; Wood, 2004).

441 In addition, the potential non-carcinogenic risks to children was found to be higher
442 than that of adults. Children might be more vulnerable than adults for ingestion rate,
443 inhalation exposure pose and dermal exposure. The exposure route through ingestion
444 was also the main way for children to face the health risks. The non-cancer risks for
445 children caused by exposure to any single metal or the exposure to six metals on road
446 dust were all below the risk threshold. However, it was worth noting that high non-
447 cancer risks exposed to six metals were undoubtedly a serious potential peril to children
448 health. Fe was the main metal causing non-cancer risk, followed by Mn and Zn, and the
449 next lower level was Pb, Cu and Cr. Obviously, compared with the high non-cancer
450 risk to children exposed in Kuala Lumpur (Wahab et al., 2020), Hubei Province (Zhang
451 et al., 2019a) and Gary (Dietrich et al., 2019) areas, the health risks to children exposed
452 in this study area were relatively low. Moreover, the main exposure route for children
453 in this study area was ingestion which was same as the investigation in Dhaka (Rahman
454 et al., 2019) and Queensland (Jayarathne et al., 2018) areas, while differed from that in
455 Serbia (Skrbic et al., 2019) which were mainly through dermal contact. It was worth
456 noting that the Hazard Quotient of metals for human was related to the number of the
457 investigated metal species and the above discussion on the non-cancer risks was based
458 on six target metals.

459 The non-carcinogenic risks for adults (Figure 2) and children (Figure S3) varied
460 significantly with seasons, and the variation pattern was basically similar. For most
461 metals, road dust in the summer posed more serious potential health risks through three
462 exposure pathways. The potential health risks in spring were notably reduced. However,
463 the risk characteristics of Cr exposure were not the same, which exhibited the highest
464 health risks in winter and the smallest risks in spring. The relatively higher metal
465 concentration on road dust in summer than in spring might be one of the important
466 causes for serious potential health risks presented in summer in this study. Another
467 important factor was probably due to the increased exposure time and exposure area of
468 human skin during the summer. Non-carcinogenic risk assessments caused by dermal
469 contact also proved that the increase in exposure area of human skin in the summer
470 greatly raised the potential health risks (Table S3a and Figure 2). There were few
471 studies on seasonal non-cancer risk assessment exposed to metals on road dust (Men et
472 al., 2020; Skrbic et al., 2019).

473 In view of the differences in population, traffic flow and human activities between
474 the functional areas, the mass of build-up particles on the road, the metal concentration
475 and the emission factors of road dust were different (Liu et al., 2019; Patton et al., 2017).
476 Except for Fe and Mn, metals on road dust in commercial areas mainly caused the
477 highest potential health risks through ingestion. The health risks caused by the ingestion
478 of metals Fe and Mn on road dust in traffic area were highest. According to the source
479 analysis, the industrial and construction activity was the main source of Fe and Mn on
480 road dust. There were always construction activities near the traffic area, which might

481 be the vital reason for the higher potential risks in traffic area. In addition, all metals in
482 the traffic area displayed the highest potential non-cancer risk through direct inhalation
483 route, which was mainly related to the large amount of suspended road dust caused by
484 the dense traffic. Fe, Mn and Zn in the traffic area, Pb and Cr in the commercial area,
485 and Cu in the residential area all posed threat to human health through dermal contact.
486 Due to the low traffic volume in residential area, the potential health risks exposed to
487 various metals through direct inhalation were relatively low. Timely road sweeping
488 carried out in central commercial street and thus the accumulated particle load was less.
489 Therefore, the health risks caused by dermal contact in central commercial street were
490 low, even if the traffic volume was heavy.

491 **2.4 Seasonal carcinogenic risk health assessment**

492 Cr and Pb were still widely used in industry and daily life, and they were
493 considered as carcinogenic elements for the Incremental Lifetime Cancer Risk (ILCR)
494 of adults and children (Table S9). ILCR between 10^{-6} and 10^{-4} was determined to be an
495 acceptable range for carcinogenic risk but could not be ignored. Exposure to metal Pb
496 on road dust through the direct inhalation route did not pose a significant cancer risk
497 for both adults and children. However, the cancer risk caused by metal Cr on road dust
498 exceeded the minimum threshold (10^{-6}) for adults and children in a probability larger
499 than 5%. Most studies have shown that Cr was within the cancer threshold (Jayarathne
500 et al., 2018; Rahman et al., 2019). These evaluation results were enough to attract people's
501 attention and take measures.

502 Adults and children exposed to Pb in road dust had relatively high potential cancer

503 risks in summer and autumn, while exposure to Cr posed comparatively high potential
504 cancer risks in winter (Figure 4). Undoubtedly, the traffic areas with a lot of road dust
505 would bring high potential cancer risks to adults and children through the direct
506 inhalation exposure route. This was followed by the central commercial area, which
507 had a relatively higher traffic volume. Identifying metals that made principal
508 contributions to human health risks in different seasons and functional areas was
509 essential to effectively recognize source control targets and improve risk control
510 efficiency.

511 **2.5 Critical sources accounting for human health risk**

512 Particular metals were believed to have special risk factors for health risks.
513 Pollutant sources that contributed a lot to the metals on road dust might not necessarily
514 have a large impact on health risks. Figure 5 depicted the contribution proportion of
515 metal sources to Hazard Index (HI) and Incremental Lifetime Cancer Risk (ILCR) for
516 adults and children in different seasons. Even if the concentration proportion of each
517 source fluctuated significantly due to the seasons, industrial and construction activity
518 was the main source for the metals on road dust (29% - 47%) and the HI of adults (27%
519 - 45%) and children (41% - 50%) in different seasons. During the study period, there
520 were a lot of construction activities near the study area. Therefore, the potential risks
521 from the construction activities to the surrounding human health could not be ignored
522 (Khademi et al., 2019; Liu et al., 2014). It is worthwhile for the government and people
523 to take active measures to reduce the risks. In addition, traffic non-exhaust emission in
524 spring and domestic waste in summer were also major sources of pollution that pose

525 potential health risks.

526 Unlike the hazard index, elements with carcinogenic risks were more likely to get
527 attention. And it was obviously that the main pollution sources for the carcinogenic
528 risks were different from the Hazard Index (Figure 5). The main source that posed
529 carcinogenic risks to adult's health in spring and summer was traffic non-exhaust
530 emission. The industrial and construction activity in winter and domestic waste in
531 autumn were important sources for the potential carcinogenic risks. Traffic non-exhaust
532 emission and industrial and construction activity also made significant contributions to
533 the potential carcinogenic risks in winter and spring, respectively. Affected by the
534 height of child, the exposure way and amount of metals for children might be different
535 from those for adults (Huang et al., 2018a). In addition, Pb and Cr posed different
536 potential carcinogenic risks for children and adults. However, the main pollution
537 sources that pose carcinogenic risks to children was similar to that of adults in different
538 seasons.

539 It was worth noting that the analysis of pollution sources in this study was only
540 based on the assessment for the carcinogenic risks of Pb and Cr. If the carcinogenic
541 risks of more metals were considered, there might be a little error in the contribution of
542 pollution sources. Considering the Hazard Index and Carcinogenic Risks, industrial
543 and construction activity and traffic non-exhaust were the critical contribution sources.
544 Identifying specific contribution sources for risk assessment is of great significance for
545 effectively controlling risk sources and reducing potential risk.

546 **3. Conclusion**

547 This study comprehensively evaluated the concentration characteristics, source
548 apportionment and health risks of metals on road dust. The metal exposure mainly
549 posed a hazard to human health through ingestion route. Pb and Mn, Fe and Mn were
550 the main harmful elements that caused non-cancer risks for adults and children,
551 respectively. The cancer risks for adults and children exposed to Cr exceeded the
552 minimum threshold. Higher cancer risks for adults and children exposed to Pb were
553 shown in summer and autumn, while shown in winter exposed to Cr. Five major
554 concentration factors were identified for the elements on road dust in different seasons
555 based on the PMF model, including atmosphere deposition, fertilizer, domestic waste,
556 industrial and construction activity, and traffic non-exhaust emission. More importantly,
557 the major contribution sources for metals on road dust and health risks for adults and
558 children in different seasons might be inconsistent. By combining the PMF model and
559 health risk models, industrial and construction activity was identified as the critical
560 source of both the pollutants on road dust (29% - 47%) and the HI for adults (27% -
561 45%) and children (41% - 50%) in different seasons. However, traffic non-exhaust
562 emission dominated in the carcinogenic risks for children and adults in spring (45%)
563 and summer (36%). Different source control regulations should be taken in different
564 seasons. It is essential for effectively identifying source control targets and
565 consequently improving risk control efficiency. Considering the impacts of the amount
566 of metals on risk assessment, more metals will be investigated in the future research.

567

568

569

570

571

572

573 **DECLARATIONS**

574 **Ethics approval and consent to participate**

575 Not applicable.

576 **Consent for publication**

577 Not applicable.

578 **Availability of data and materials**

579 The authors declare that all the datasets generated during and/or analysed during
580 the current study are available in the article and its SI Appendix.

581 **Competing interests**

582 The authors declare that they have no competing interests.

583 **Funding**

584 This work was supported by the National Water Pollution Control and Treatment
585 Science and Technology Major Project of China (2017ZX07106001).

586 **Authors' contributions**

587 Jingshu Wang: put forward ideas, performed the experiments and wrote the initial
588 draft.

589 Jinhui Jeanne Huang: provided study materials, reagents and materials, supervised
590 research activity, and revised draft.

592 **References**

- 593 Alves, S.P., Alfaia, C.M., Škrbić, B.D., Živančev, J.R., Fernandes, M.J., Bessa, R.J.B.
594 and Fraqueza, M.J. 2017. Screening chemical hazards of dry fermented
595 sausages from distinct origins: Biogenic amines, polycyclic aromatic
596 hydrocarbons and heavy elements. *Journal of Food Composition and Analysis*
597 59, 124-131.
- 598 Asheim, J., Vike-Jonas, K., Gonzalez, S.V., Lierhagen, S., Venkatraman, V., Veivag,
599 I.L.S., Snilsberg, B., Flaten, T.P. and Asimakopoulos, A.G. 2019.
600 Benzotriazoles, benzothiazoles and trace elements in an urban road setting in
601 Trondheim, Norway: Re-visiting the chemical markers of traffic pollution. *Sci.*
602 *Total Environ.* 649, 703-711.
- 603 Banerjee, A.D.K. 2003. Heavy metal levels and solid phase speciation in street
604 dusts of Delhi, India. *Environ. Pollut.* 123(1), 95-105.
- 605 Bourliva, A., Papadopoulou, L. and Aidona, E. 2016. Study of road dust magnetic
606 phases as the main carrier of potentially harmful trace elements. *Sci. Total*
607 *Environ.* 553, 380-391.
- 608 Bzdusek, P.A., Christensen, E.R., Li, A. and Zou, Q. 2004. Source Apportionment
609 of Sediment PAHs in Lake Calumet, Chicago: Application of Factor Analysis
610 with Nonnegative Constraints. *Environ. Sci. Technol.* 38(1), 97-103.
- 611 Charlesworth, S., Everett, M., McCarthy, R., Ordóñez, A. and de Miguel, E. 2003.
612 A comparative study of heavy metal concentration and distribution in deposited
613 street dusts in a large and a small urban area: Birmingham and Coventry, West

614 Midlands, UK. *Environment International* 29(5), 563-573.

615 CNEMC China National Environmental Monitoring Center. *The Backgrounds of*
616 *Soil Environment in China*. 1990. Environment Science Press of China.

617 Deletic, A. and Orr, D.W. 2005. Pollution buildup on road surfaces. *J. Environ.*
618 *Eng.-ASCE* 131(1), 49-59.

619 Dietrich, M., Wolfe, A., Burke, M. and Krekeler, M.P.S. 2019. The first pollution
620 investigation of road sediment in Gary, Indiana: Anthropogenic metals and
621 possible health implications for a socioeconomically disadvantaged area.
622 *Environment International* 128, 175-192.

623 EPA, U.S. 1989. *Risk Assessment Guidance for Superfund, vol. I: Human Health*
624 *Evaluation Manual*. EPA/540/1-89/002. Office of Solid Waste and Emergency
625 *Response*. US Environmental Protection Agency. Washington, D.C. .

626 EPA, U.S. 2001a. *Risk Assessment Guidance for Superfund: Volume III - Part A,*
627 *Process for Conducting Probabilistic Risk Assessment (EPA 540-R-02-002).*
628 [U.S. Environmental Protection Agency].

629 EPA, U.S. 2001b. *Supplemental Guidance for Developing Soil Screening Levels*
630 *for Superfund Sites*. OSWER 9355.4-24. Office of Solid Waste and Emergency
631 *Response*. U.S. Environmental Protection Agency. Washington, D.C

632 EPA, U.S. 2004. *Risk Assessment Guidance for Superfund Volume I: Human*
633 *Health Evaluation Manual (Part E, Supplemental Guidance for Dermal Risk*
634 *Assessment)*. OSWER 9285.7-02EP. Office of Solid Waste and Emergency
635 *Response*. U.S. Environmental Protection Agency. Washington, D.C.

636 EPA, U.S. 2009a. Risk Assessment Guidance for Superfund Volume I: Human Health
637 Evaluation Manual (Part F, Supplemental Guidance for Inhalation Risk
638 Assessment). Office of Superfund Remediation and Technology Innovation,
639 U.S. Environmental Protection Agency.

640 EPA, U.S. 2009b. Application of Bioavailability in the Assessment of Human Health
641 Hazards and Cancer Risk. Division of Environmental Response and
642 Revitalization, Ohio Environmental Protection Agency, Columbus, OH, p. 4.

643 Feng, T., Bei, N., Zhao, S., Wu, J., Liu, S., Li, X., Liu, L., Wang, R., Zhang, X., Tie, X.
644 and Li, G. 2021. Nitrate debuts as a dominant contributor to particulate
645 pollution in Beijing: Roles of enhanced atmospheric oxidizing capacity and
646 decreased sulfur dioxide emission. *Atmospheric Environment* 244, 117995.

647 Fergusson, J.E. and Ryan, D.E. 1984. The elemental composition of street dust from
648 large and small urban areas related to city type, source and particle size. *Sci.*
649 *Total Environ.* 34(1), 101-116.

650 Gavrić, S., Leonhardt, G., Marsalek, J. and Viklander, M. 2019. Processes
651 improving urban stormwater quality in grass swales and filter strips: A review
652 of research findings. *Sci. Total Environ.* 669, 431-447.

653 Gbeddy, G., Jayarathne, A., Goonetilleke, A., Ayoko, G.A. and Egodawatta, P. 2018.
654 Variability and uncertainty of particle build-up on urban road surfaces. *Sci. Total*
655 *Environ.* 640-641, 1432-1437.

656 Ghafourian, K., Shapiro, J.S., Goodman, L. and Ardehali, H. 2020. Iron and
657 Heart Failure: Diagnosis, Therapies, and Future Directions. *JACC: Basic to*

658 Translational Science 5(3), 300-313.

659 Giroux, M., Esclassan, J., Arnaud, C. and Chalé, J.J. 1997. Analysis of levels of
660 nitrates and derivatives of ammonia in an urban atmosphere. *Sci. Total Environ.*
661 196(3), 247-254.

662 Gunawardana, C., Egodawatta, P. and Goonetilleke, A. 2014. Role of particle size
663 and composition in metal adsorption by solids deposited on urban road surfaces.
664 *Environ. Pollut.* 184, 44-53.

665 Hong, N., Guan, Y., Yang, B., Zhong, J., Zhu, P., Ok, Y.S., Hou, D., Tsang, D.C.W.,
666 Guan, Y. and Liu, A. 2020. Quantitative source tracking of heavy metals
667 contained in urban road deposited sediments. *J. Hazard. Mater.* 393, 122362.

668 Hou, S., Zheng, N., Tang, L., Ji, X., Li, Y. and Hua, X. 2019. Pollution
669 characteristics, sources, and health risk assessment of human exposure to Cu,
670 Zn, Cd and Pb pollution in urban street dust across China between 2009 and
671 2018. *Environment International* 128, 430-437.

672 Hu, X., Zhang, Y., Luo, J., Wang, T., Lian, H. and Ding, Z. 2011. Bioaccessibility
673 and health risk of arsenic, mercury and other metals in urban street dusts from
674 a mega-city, Nanjing, China. *Environ. Pollut.* 159(5), 1215-1221.

675 Huang, J., Guo, S., Zeng, G.-m., Li, F., Gu, Y., Shi, Y., Shi, L., Liu, W. and Peng, S.
676 2018a. A new exploration of health risk assessment quantification from
677 sources of soil heavy metals under different land use. *Environ. Pollut.* 243, 49-
678 58.

679 Huang, R.J., Cheng, R., Jing, M., Yang, L., Li, Y., Chen, Q., Chen, Y., Yan, J., Lin, C.,

680 Wu, Y., Zhang, R., El Haddad, I., Prevot, A.S.H., O'Dowd, C.D. and Cao, J.
681 2018b. Source-Specific Health Risk Analysis on Particulate Trace Elements:
682 Coal Combustion and Traffic Emission As Major Contributors in Wintertime
683 Beijing. *Environ Sci Technol* 52(19), 10967-10974.

684 Huang, Y., Deng, M., Wu, S., Japenga, J., Li, T., Yang, X. and He, Z. 2018c. A
685 modified receptor model for source apportionment of heavy metal pollution in
686 soil. *J Hazard Mater* 354, 161-169.

687 Jayarathne, A., Egodawatta, P., Ayoko, G.A. and Goonetilleke, A. 2018.
688 Assessment of ecological and human health risks of metals in urban road dust
689 based on geochemical fractionation and potential bioavailability. *Sci. Total*
690 *Environ.* 635, 1609-1619.

691 Khademi, H., Gabarron, M., Abbaspour, A., Martinez-Martinez, S., Faz, A. and Acosta,
692 J.A. 2019. Environmental impact assessment of industrial activities on
693 heavy metals distribution in street dust and soil. *Chemosphere* 217, 695-705.

694 Lin, Y., Qiu, X., Ma, Y., Ma, J., Zheng, M. and Shao, M. 2015. Concentrations and
695 spatial distribution of polycyclic aromatic hydrocarbons (PAHs) and nitrated
696 PAHs (NPAHs) in the atmosphere of North China, and the transformation from
697 PAHs to NPAHs. *Environ. Pollut.* 196, 164-170.

698 Liu, A., Hong, N., Zhu, P. and Guan, Y. 2018. Understanding benzene series (BTEX)
699 pollutant load characteristics in the urban environment. *Sci. Total Environ.* 619-
700 620, 938-945.

701 Liu, A., Hong, N.A., Zhu, P.F. and Guan, Y.T. 2019. Characterizing petroleum

702 hydrocarbons deposited on road surfaces in urban environments. *Sci. Total*
703 *Environ.* 653, 589-596.

704 Liu, E., Yan, T., Birch, G. and Zhu, Y. 2014. Pollution and health risk of potentially
705 toxic metals in urban road dust in Nanjing, a mega-city of China. *Sci Total*
706 *Environ* 476-477, 522-531.

707 Liu, G.-R., Peng, X., Wang, R.-K., Tian, Y.-Z., Shi, G.-L., Wu, J.-H., Zhang, P., Zhou,
708 L.-D. and Feng, Y.-C. 2015. A new receptor model-incremental lifetime
709 cancer risk method to quantify the carcinogenic risks associated with sources of
710 particle-bound polycyclic aromatic hydrocarbons from Chengdu in China. *J.*
711 *Hazard. Mater.* 283, 462-468.

712 Men, C., Liu, R., Wang, Q., Guo, L., Miao, Y. and Shen, Z. 2019. Uncertainty
713 analysis in source apportionment of heavy metals in road dust based on positive
714 matrix factorization model and geographic information system. *Sci. Total*
715 *Environ.* 652, 27-39.

716 Men, C., Liu, R., Wang, Q., Guo, L. and Shen, Z. 2018. The impact of seasonal
717 varied human activity on characteristics and sources of heavy metals in
718 metropolitan road dusts. *Sci. Total Environ.* 637, 844-854.

719 Men, C., Liu, R., Xu, L., Wang, Q., Guo, L., Miao, Y. and Shen, Z. 2020. Source-
720 specific ecological risk analysis and critical source identification of heavy
721 metals in road dust in Beijing, China. *J. Hazard. Mater.* 388, 121763.

722 Ministry of Ecology and Environment, P. 2013. *Exposure Factors Handbook of*
723 *Chinese Population.* China Environment Publishing Group.

724 Paatero, P. and Tapper, U. 1994. Positive matrix factorization: A non-negative factor
725 model with optimal utilization of error estimates of data values. *Environmetrics*
726 5(2), 111-126.

727 Pateraki, S., Manousakas, M., Bairachtari, K., Kantarelou, V., Eleftheriadis, K.,
728 Vasilakos, C., Assimakopoulos, V.D. and Maggos, T. 2019. The traffic
729 signature on the vertical PM profile: Environmental and health risks within an
730 urban roadside environment. *Sci. Total Environ.* 646, 448-459.

731 Patton, A.P., Milando, C., Durant, J.L. and Kumar, P. 2017. Assessing the
732 Suitability of Multiple Dispersion and Land Use Regression Models for Urban
733 Traffic-Related Ultrafine Particles. *Environ. Sci. Technol.* 51(1), 384-392.

734 Rahman, M.S., Khan, M.D.H., Jolly, Y.N., Kabir, J., Akter, S. and Salam, A. 2019.
735 Assessing risk to human health for heavy metal contamination through street
736 dust in the Southeast Asian Megacity: Dhaka, Bangladesh. *Sci. Total Environ.*
737 660, 1610-1622.

738 Rasmussen, P.E., Subramanian, K.S. and Jessiman, B.J. 2001. A multi-element
739 profile of house dust in relation to exterior dust and soils in the city of Ottawa,
740 Canada. *Sci. Total Environ.* 267(1), 125-140.

741 Rhee, H.-P., Yoon, C.G., Lee, S.-J., Choi, J.-H. and Son, Y.-K. 2012. Analysis of
742 Nonpoint Source Pollution Runoff from Urban Land Uses in South Korea.
743 *Environmental Engineering Research* 17(1), 47-56.

744 Robertson, D.J., Taylor, K.G. and Hoon, S.R. 2003. Geochemical and mineral
745 magnetic characterisation of urban sediment particulates, Manchester, UK. *Appl.*

746 Geochem. 18(2), 269-282.

747 Salim, I., Sajjad, R.U., Paule-Mercado, M.C., Memon, S.A., Lee, B.-Y., Sukhbaatar, C.
748 and Lee, C.-H. 2019. Comparison of two receptor models PCA-MLR and
749 PMF for source identification and apportionment of pollution carried by runoff
750 from catchment and sub-watershed areas with mixed land cover in South Korea.
751 Sci. Total Environ. 663, 764-775.

752 Shi, G., Chen, Z., Xu, S., Zhang, J., Wang, L., Bi, C. and Teng, J. 2008. Potentially
753 toxic metal contamination of urban soils and roadside dust in Shanghai, China.
754 Environ. Pollut. 156(2), 251-260.

755 Skrbic, B., Durisic-Mladenovic, N., Zivancev, J. and Tadic, D. 2019. Seasonal
756 occurrence and cancer risk assessment of polycyclic aromatic hydrocarbons in
757 street dust from the Novi Sad city, Serbia. Sci. Total Environ. 647, 191-203.

758 Škrbić, B.D., Kadokami, K. and Antić, I. 2018. Survey on the micro-pollutants
759 presence in surface water system of northern Serbia and environmental and
760 health risk assessment. Environmental Research 166, 130-140.

761 Sutherland, R.A. and Tolosa, C.A. 2000. Multi-element analysis of road-deposited
762 sediment in an urban drainage basin, Honolulu, Hawaii. Environ. Pollut. 110(3),
763 483-495.

764 Tian, S., Liang, T. and Li, K. 2019. Fine road dust contamination in a mining area
765 presents a likely air pollution hotspot and threat to human health. Environment
766 International 128, 201-209.

767 Tomašević, M., Vukmirović, Z., Rajšić, S., Tasić, M. and Stevanović, B. 2005.

768 Characterization of trace metal particles deposited on some deciduous tree
769 leaves in an urban area. *Chemosphere* 61(6), 753-760.

770 Wahab, M.I.A., Abd Razak, W.M.A., Sahani, M. and Khan, M.F. 2020.
771 Characteristics and health effect of heavy metals on non-exhaust road dusts in
772 Kuala Lumpur. *Sci. Total Environ.* 703, 11.

773 Wang, J., Huang, J.J. and Li, J. 2019a. A study of the road sediment build-up
774 process over a long dry period in a megacity of China. *Sci. Total Environ.* 696,
775 133788.

776 Wang, J., Huang, J.J. and Li, J. 2020. Characterization of the pollutant build-up
777 processes and concentration/mass load in road deposited sediments over a long
778 dry period. *Sci. Total Environ.* 718, 137282.

779 Wang, S., Cai, L.-M., Wen, H.-H., Luo, J., Wang, Q.-S. and Liu, X. 2019b. Spatial
780 distribution and source apportionment of heavy metals in soil from a typical
781 county-level city of Guangdong Province, China. *Sci. Total Environ.* 655, 92-
782 101.

783 Wang, W., Yu, J., Cui, Y., He, J., Xue, P., Cao, W., Ying, H., Gao, W., Yan, Y., Hu, B.,
784 Xin, J., Wang, L., Liu, Z., Sun, Y., Ji, D. and Wang, Y. 2018. Characteristics
785 of fine particulate matter and its sources in an industrialized coastal city, Ningbo,
786 Yangtze River Delta, China. *Atmospheric Research* 203, 105-117.

787 Wijaya, A.R., Ouchi, A.K., Tanaka, K., Shinjo, R. and Ohde, S. 2012. Metal
788 contents and Pb isotopes in road-side dust and sediment of Japan. *Journal of*
789 *Geochemical Exploration* 118, 68-76.

790 Wijesiri, B., Egodawatta, P., McGree, J. and Goonetilleke, A. 2016. Understanding
791 the uncertainty associated with particle-bound pollutant build-up and wash-off:
792 A critical review. *Water Res.* 101, 582-596.

793 Wood, R.J. 2004. The iron–heart disease connection: is it dead or just hiding?
794 *Ageing Research Reviews* 3(3), 355-367.

795 Yang, T., Liu, Q., Li, H., Zeng, Q. and Chan, L. 2010. Anthropogenic magnetic
796 particles and heavy metals in the road dust: Magnetic identification and its
797 implications. *Atmospheric Environment* 44(9), 1175-1185.

798 Yongming, H., Peixuan, D., Junji, C. and Posmentier, E.S. 2006. Multivariate
799 analysis of heavy metal contamination in urban dusts of Xi'an, Central China.
800 *Sci. Total Environ.* 355(1), 176-186.

801 Yu, B., Wang, Y. and Zhou, Q. 2014. Human Health Risk Assessment Based on
802 Toxicity Characteristic Leaching Procedure and Simple Bioaccessibility
803 Extraction Test of Toxic Metals in Urban Street Dust of Tianjin, China. *PLOS*
804 *ONE*.

805 Zhang, H., Mao, Z., Huang, K., Wang, X., Cheng, L., Zeng, L., Zhou, Y. and Jing, T.
806 2019a. Multiple exposure pathways and health risk assessment of heavy
807 metal(loid)s for children living in fourth-tier cities in Hubei Province.
808 *Environment International* 129, 517-524.

809 Zhang, J., Li, R.F., Zhang, X.Y., Bai, Y., Cao, P. and Hua, P. 2019b. Vehicular
810 contribution of PAHs in size dependent road dust: A source apportionment by
811 PCA-MLR, PMF, and Unmix receptor models. *Sci. Total Environ.* 649, 1314-

812 1322.

813 Zhang, K. and Batterman, S. 2013. Air pollution and health risks due to vehicle
814 traffic. *Sci. Total Environ.* 450-451, 307-316.

815 Zhao, H.T., Shao, Y.P., Yin, C.Q., Jiang, Y. and Li, X.Y. 2016. An index for
816 estimating the potential metal pollution contribution to atmospheric particulate
817 matter from road dust in Beijing. *Sci. Total Environ.* 550, 167-175.

818 Zhao, J., Ji, Y., Li, Y., Zhang, I. and Wang, S. 2019. Distribution Characteristics of
819 Traffic Volume for Typical Roads in Tianjin City. *Research of Environmental
820 Sciences.* 32(3): 399-405.

821 Zhao, L., Xu, Y., Hou, H., Shangguan, Y. and Li, F. 2014. Source identification and
822 health risk assessment of metals in urban soils around the Tanggu chemical
823 industrial district, Tianjin, China. *Sci. Total Environ.* 468-469, 654-662.

824 Zheng, N., Liu, J., Wang, Q. and Liang, Z. 2010. Health risk assessment of heavy
825 metal exposure to street dust in the zinc smelting district, Northeast of China.
826 *Sci. Total Environ.* 408(4), 726-733.

827 Živančev, J.R., Ji, Y., Škrbić, B.D. and Buljovčić, M.B. 2019. Occurrence of heavy
828 elements in street dust from sub/urban zone of Tianjin: pollution characteristics
829 and health risk assessment. *Journal of Environmental Science and Health, Part
830 A* 54(10), 999-1010.

831

Table 1. Relative contributions of the measured elements on road dust to the factors (1-5) in different seasons.

	Spring (%)					Summer (%)					Autumn (%)					Winter (%)				
	F1	F2	F3	F4	F5	F1	F2	F3	F4	F5	F1	F2	F3	F4	F5	F1	F2	F3	F4	F5
Fe	6.7	8.1	18.4	41.6	25.3	14.5	3.1	34.8	47.7	0	29.8	17.3	8	44.5	0	18.7	8.4	2.9	50	20
Pb	0	10.4	6.4	37	46.2	16.2	0	36.2	14.4	33.3	19.8	24.6	20	17.5	18	13.1	4.5	3.8	39.1	39.5
Cu	9.6	0	27.7	31.2	31.4	22.1	5.7	36.6	21.9	13.8	17.6	14.7	16.8	40.4	10.5	14.4	3.6	0	49.9	31.8
Zn	5.9	14.8	10	26	43.4	16.5	10	37.3	9.3	26.9	0	0	8	40.5	51.4	16.6	1.3	0	46	36.1
Cr	3.9	4.6	8.5	39	44.1	7.8	17.2	0	36.5	38.5	11	27.4	37.4	24.2	0	21.1	0	3.8	45.5	29.6
Mn	0	12.5	21.1	49.2	17.2	13.2	6.8	28.7	43.2	8.1	32.4	20.1	0	42.4	5.2	22.3	9	2.2	50	16.5
TOC	15.7	2.4	53.1	9.4	19.4	0	10	74	0	16	0	41.8	57.8	0	0	0	1	44.5	23.5	31
NH ₃ -N	22.6	48.6	11.3	0	17.6	13.9	28.3	21.9	19.4	16.4	24.7	36.3	16.3	15.7	7.1	22.9	0	0	59	18.1
NO ₃ -N	65.9	1.1	0	33.1	0	60.2	31.4	8.4	0	0	71.1	0	21.3	0	7.3	74.2	2.8	23	0	0
TP	11.2	7.9	26.6	26.2	28.1	0	61.3	20.9	0	17.1	22.6	53.2	0	0	24.1	11.1	61.3	0	0	27.6

Figure captions

Figure 1. Histogram of metal concentrations on road dust in different seasons and functional areas (including metal concentrations for different size particles). JM, JT, SY and BJ represent residential area, traffic area, commercial area and central commercial street, respectively.

Figure 2. Contribution of metals to non-carcinogenic risks of adult through three exposure pathways in different seasons.

Figure 3. Contribution of metals to non-carcinogenic risks of adult through three exposure pathways in different functional areas.

Figure 4. Carcinogenic elements display potential health risks to adults and children in different seasons and functional areas.

Figure 5. Source contributions of metals to Hazard Index (HI) and Incremental Lifetime Cancer Risk (ILCR) for adults and children in different seasons. a) HI for child; b) HI for adult; c) LICR for child; d) LICR for adult.

Figures

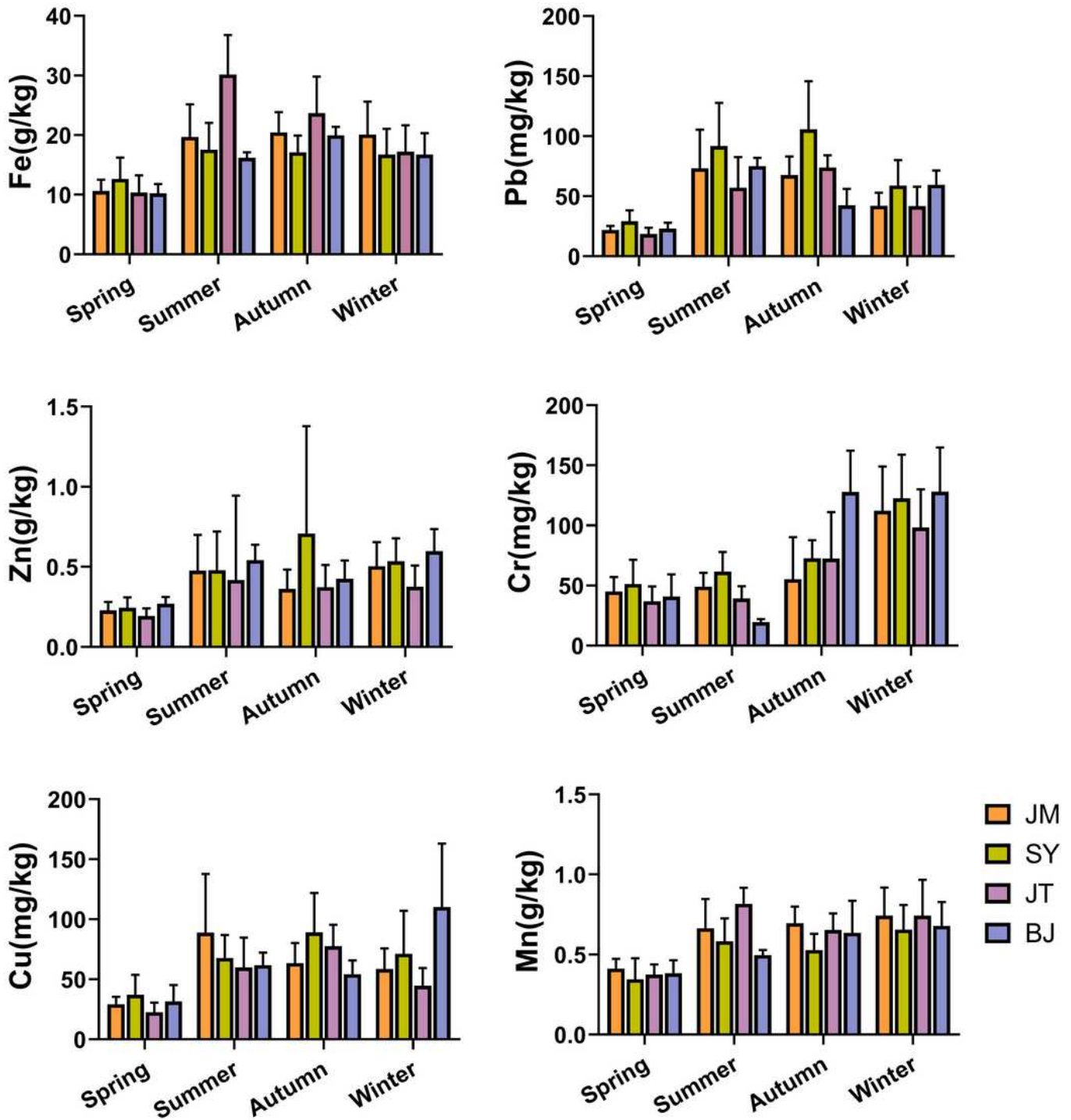


Figure 1

Histogram of metal concentrations on road dust in different seasons and functional areas (including metal concentrations for different size particles). JM, JT, SY and BJ represent residential area, traffic area, commercial area and central commercial street, respectively.

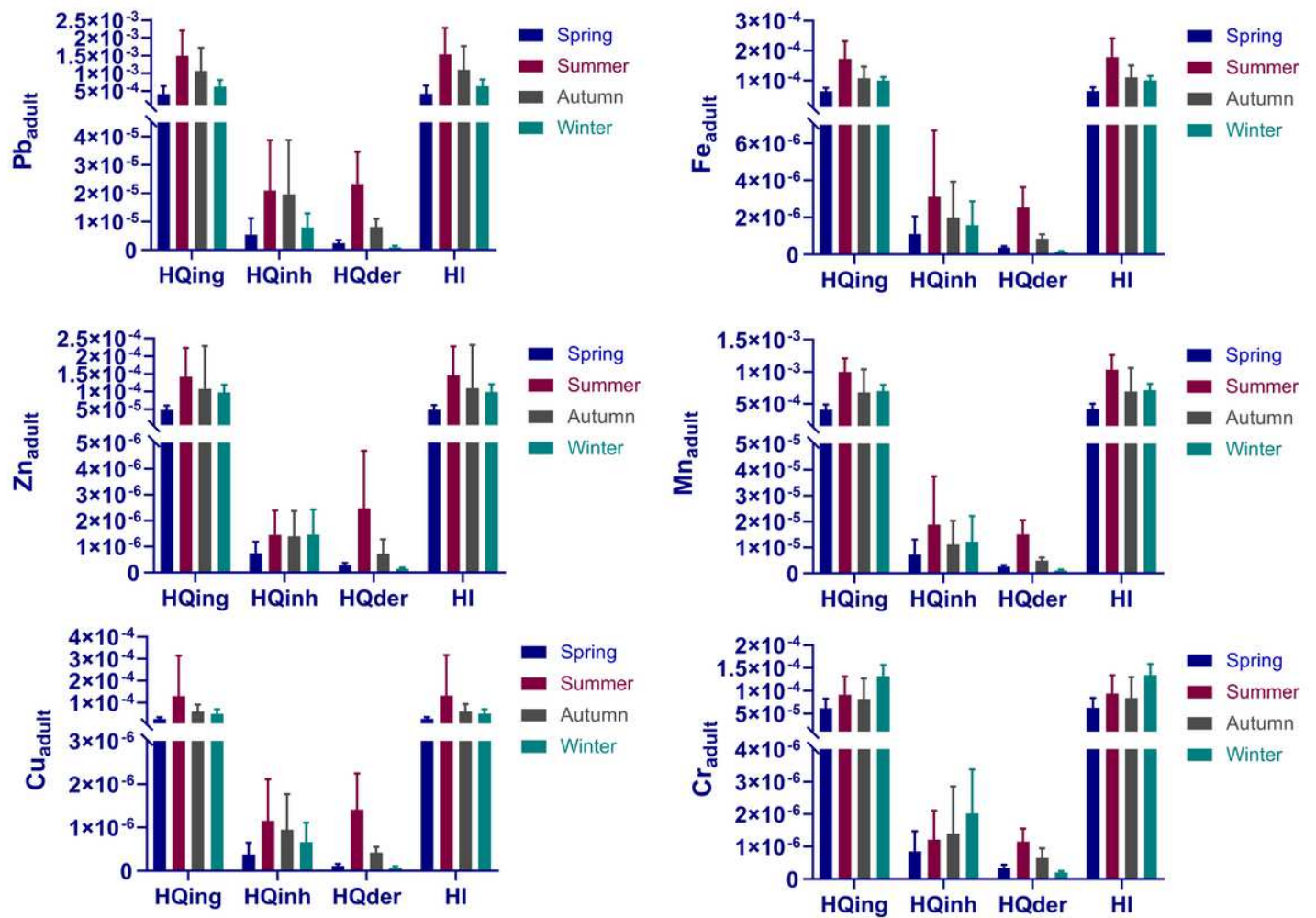


Figure 2

Contribution of metals to non-carcinogenic risks of adult through three exposure pathways in different seasons.

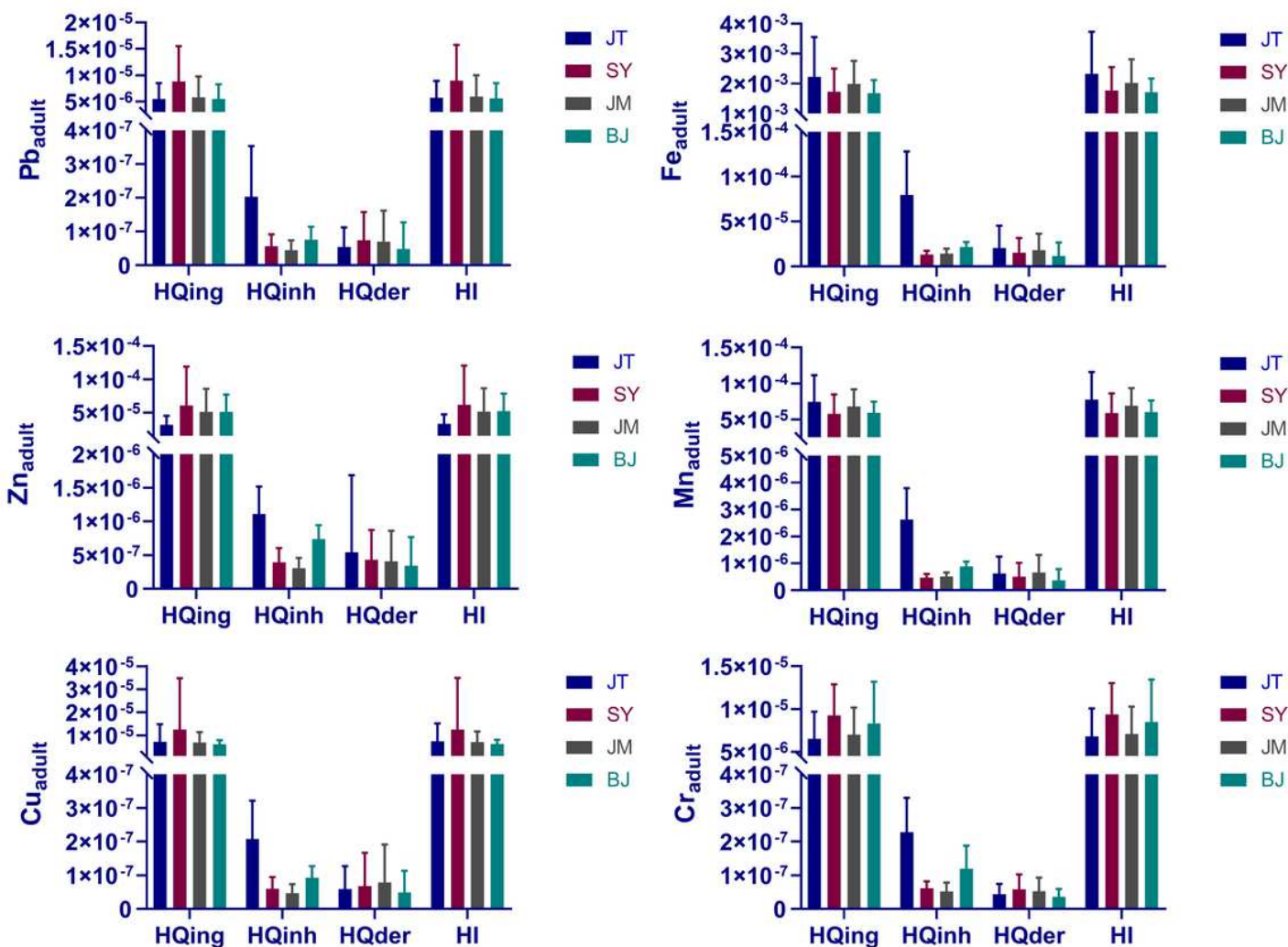


Figure 3

Contribution of metals to non-carcinogenic risks of adult through three exposure pathways in different functional areas.

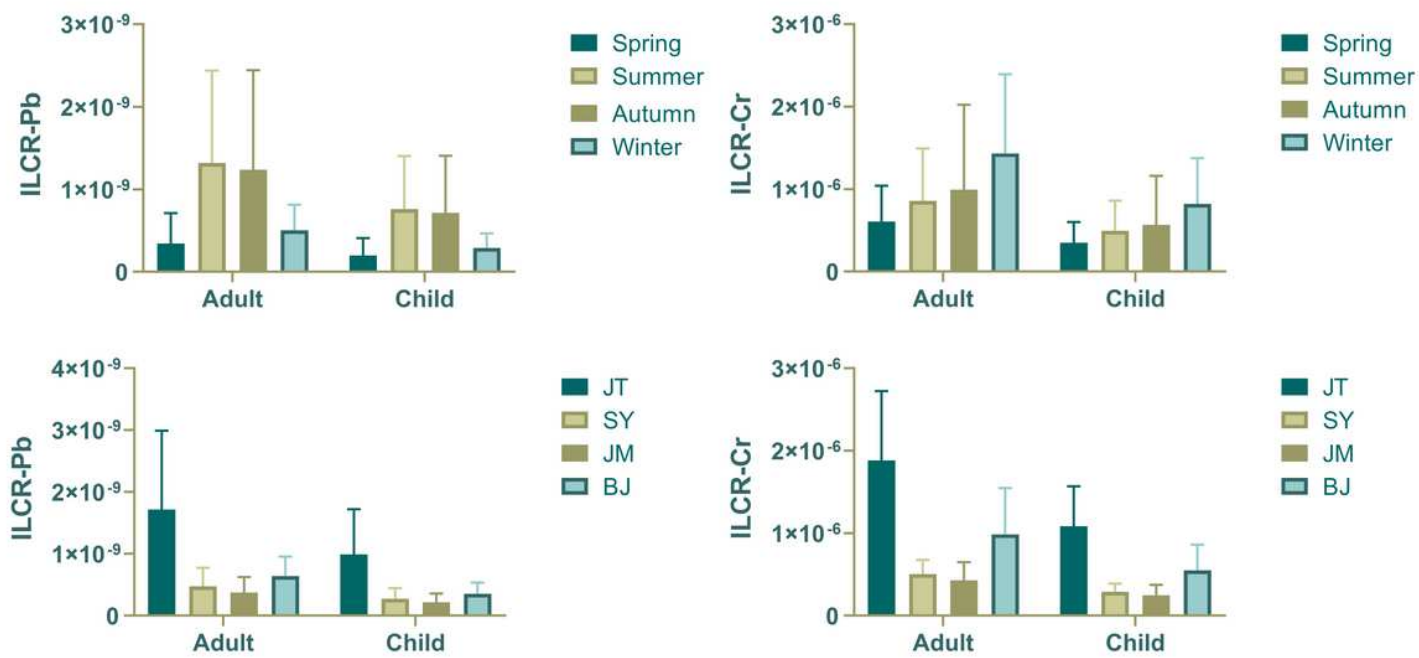


Figure 4

Carcinogenic elements display potential health risks to adults and children in different seasons and functional areas.

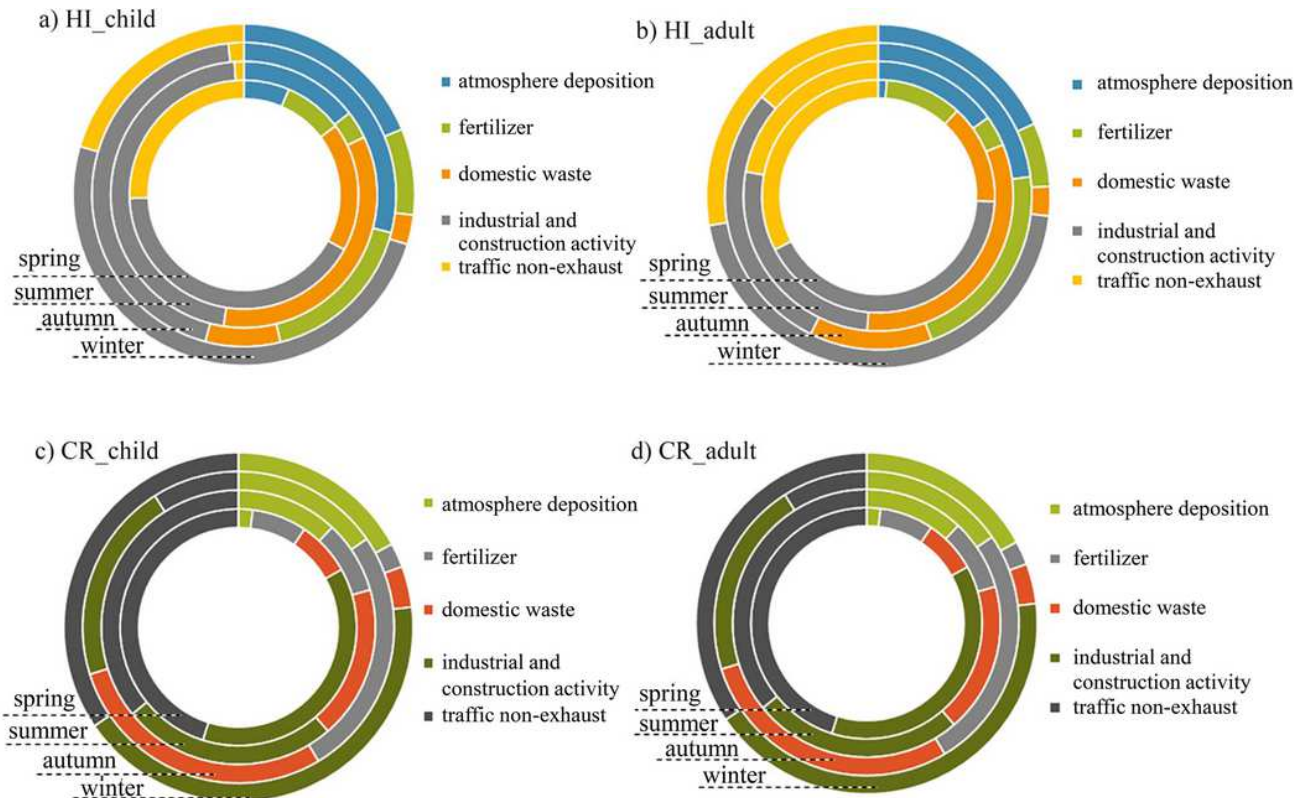


Figure 5

Source contributions of metals to Hazard Index (HI) and Incremental Lifetime Cancer Risk (ILCR) for adults and children in different seasons. a) HI for child; b) HI for adult; c) LICR for child; d) LICR for adult.

Supplementary Files

This is a list of supplementary files associated with this preprint. Click to download.

- [SI.docx](#)